Short-Term Variability of Wind Measurements in South China Sea

Joel Muyau, Sarawak Shell Bhd, Kevin Ewans, Sarawak Shell Bhd, and Philip Jonathan, Shell Global Solutions

Abstract

Good understanding of the wind characteristics is essential in offshore structural design and operational activities. The short-term variability of wind is captured in design codes with prescribed forms for the wind spectrum and for the ratio of mean wind speed maxima for given durations to the one hour mean. Relationships are also prescribed for scaling these wind speeds between different elevations, essentially defining the wind profile in the turbulent boundary layer. All of these are based largely on measurements made in mid-latitude regions during extra-tropical storms or hurricanes; but these measurements will not be representative of the wind field during squalls, which are not stationary, and possibly not representative of the wind field during general monsoonal conditions. Several years of continuous recordings of wind speed and direction, sampled at 1Hz, at several South China Sea locations allow us to examine the short-term variability of wind in squalls and monsoonal conditions, and allow comparison with expressions given in design codes. We investigate the variability of the stationarity of the winds, the wind spectrum, the mean wind speed, and the wind profile, for the South China Sea measurements. The premise for the short-term variability prescriptions is that the wind field is stationary. Accordingly, we first report our evaluation of this assumption, and based on this, our evaluation of the relevance of the various prescriptions in the codes for describing short-term variability is developed.

1.0 Introduction

An accurate specification of the wind is an essential element of the metocean design criteria for oil and gas facilities both offshore and onshore. In particular, a good understanding of the wind characteristic specific to a given location can provide considerable economical benefit as well as ensuring integrity of the designed structures.

An informative description of the wind variability is provided by Van der Hoven (1957), who estimated the wind power spectrum from wind measurements made at Brookhaven National Laboratory, Long Island, New York. His spectral plot, reproduced in Figure 1, shows large peaks with periods of around 1 minute and 4 days, corresponding short-term variability associated with the gustiness of the steady wind and the long-term variability associated with the periodicity of weather systems. A smaller peak with a period of 12 hours is also apparent, presumably associated with the land-sea breeze. Similar spectral behaviour has been observed at other locations around the world both onshore and offshore (Harper *et al.*, 2009), but it can be expected that the periodicity that Van der Hoven identified in his data, particularly that associated with the long-term variability is a function of location, with each location dominated by the occurrence of different storm types. For example, at mid-latitude locations, the periodicity of extra-tropical storms might be seven to ten days, while much longer periods will be associated with tropical cyclones, and shorter-period peaks might be expected at locations that experience thunderstorms regularly.

The long-term variability is a consequence of the wind climate of the location of interest and the and the extremes of the "storminess" is expressed in design criteria as extremal statistics of the mean wind speed, usually the one-hour mean wind speed with a given return period. The short-term variability of wind is a consequence of the local turbulence, and while dependent on location specific surface roughness and perhaps storm-type, it is believed that this variability is more or less universal and is captured in design codes with, for example, prescribed forms for the wind spectrum and for the ratio of mean wind speed maxima for given durations to the one hour mean. Relationships are also prescribed for scaling these wind speeds between different elevations, essentially defining the wind profile in the turbulent boundary layer.

However, the design codes are based largely on measurements made in mid-latitude regions during extra-tropical storms or hurricanes. For example, the wind relationships in the ISO (2012) standard for offshore structural design is based on the analysis of data measured on the Island of Frøya off the Norwegian coast, and these same have also been adopted by API (2007), for hurricane conditions, but it is not clear that these measurements will not be representative of the wind field during monsoons in the South China Sea (SCS), and they will generally not be applicable to squalls, which are not stationary.
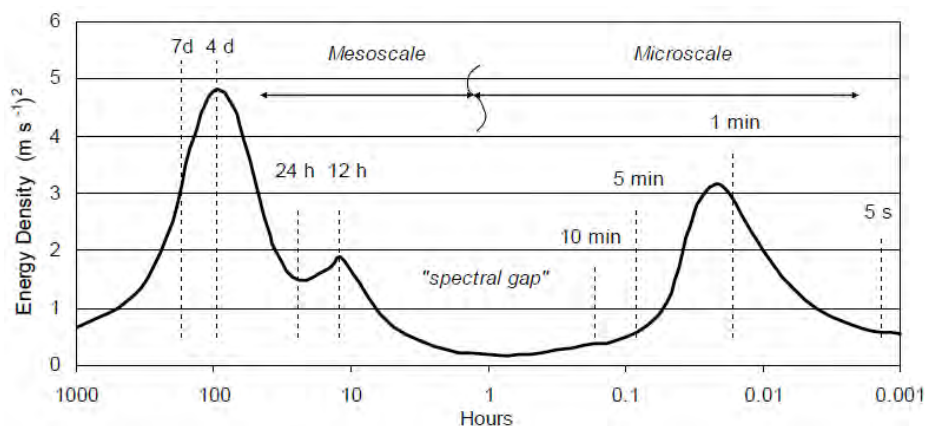

Figure 1: Schematic energy spectrum of near-ground wind speed *after Van der Hoven (1957)*.

In this paper, we investigate these short-term effects, essentially focusing our attention on the wind features that contribute to the short-period peak in Figure 1. The wind speed variability here is a consequence of the turbulence that corresponds to local surface features, such as roughness, the local atmospheric boundary layer, and the storm type.

Availability of high frequency, long and continuous dataset from several locations in SCS, discussed in Section 2, provides the opportunity to study the short term variability of the local wind. The analysis methods we have employed on the data are described in Section 3. In Section 4 we present the results, including an assessment of the wind stationarity assumption that is implicit in the short-term variability prescriptions, our estimates of the wind spectra, and gust ratios, and the wind profile. We summarise the results in Section 5.

2.0 Wind Data Source

The dataset used in this study was based on wind measurements from the SCS, predominantly from offshore locations on the western coast of Borneo, but also one onshore location, in Miri. Table 1 summarises the weather station locations and also wind sensor information. The anemometers were all Gill Wind Observer II units, and all the measurements were sampled at

1.0 Hz.

Station ID	Longitude (°E)	Latitude (°N)	Sensor Height (m)	Sensor Location
Station A (E11)	112° 40' 41.66"	4° 20' 4.02"	82	NE Telecom Tower
Station B (F23)	112° 29' 26.87"	4° 41' 19.78"	50	NE Telecom Tower
Station C (SF)	116° 13' 34.34"	6° 46' 38.85"	47	NE Helideck Corner
Station D (Miri)	114° 00' 20.88"	4° 28' 06.96"	15, 33, 45, 57, 75	S Telecom Tower

Table 1: Weather station and wind sensor locations.

Long term measurements spanning a number of years are available for each location, but due to time constraints we have only analysed a relatively small data set from each location. We used the data recorded for January 2011 for the stationarity and spectral analysis; but, our investigation of the mean wind and wind profile was based on wind measurements for all of 2010 at Station D, as this is the only station for which there are data at different elevations, having anemometers at five elevations on the same tower, at 15.2 m, 32.7 m, 44.7 m, 56.8 m, and 74.5 m.

The tower at Station D is adjacent to the Shell office in Lutong, Miri. Figure 2 shows the shows the relative locations of buildings in the proximity of the tower, including the main Shell office block, which is about 30 metres high and is situated about 80 metres to the north, and the communications hut, which is 6 metres high about 10 metres northwest of the tower. Thus, the wind flow from the northwest and north will be disturbed by the presence of these building, particularly the wind measured by the anemometer at 15.2 m elevation. The other directions are relatively free of obstructions.
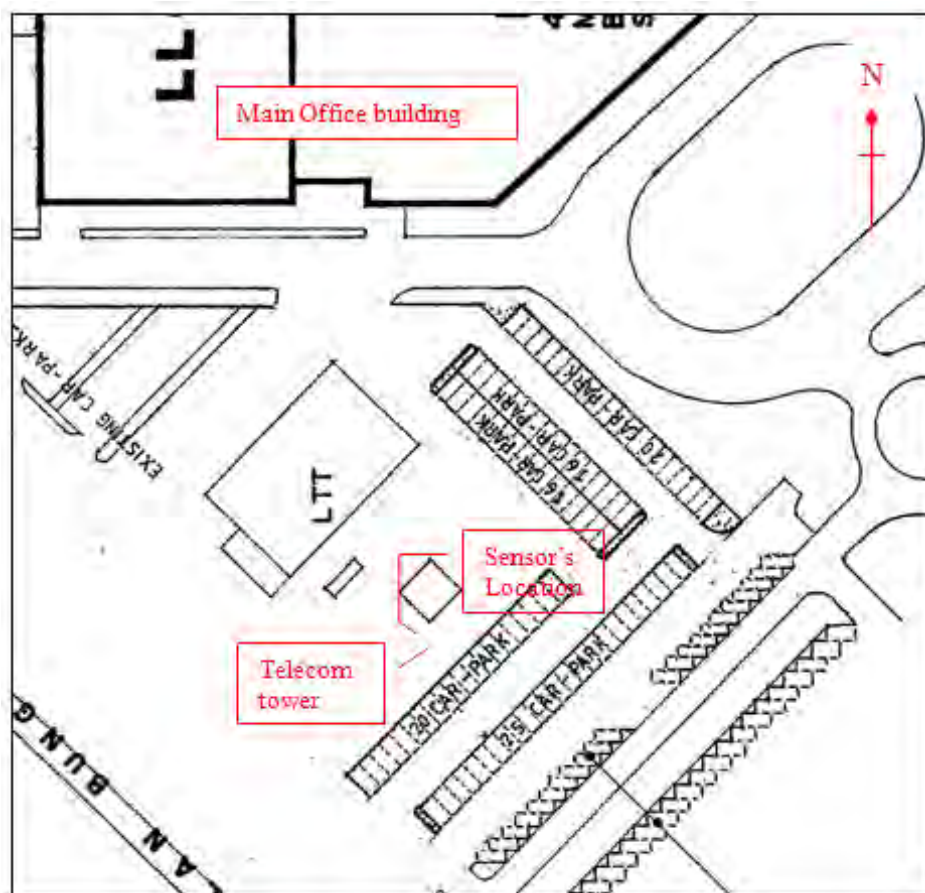

Figure 2: Illustration of the telecom tower surroundings at Station D. The wind sensors are attached to the telecom tower on the southern side.

3.0 Method

In the following, the distinction is made between mean wind speed and maximum gust, over a specific interval, and these are best considered by way of example. Suppose, as we do in this study, have wind samples at 1.0 Hz over a one-hour period, during which we consider the wind to be stationary. If we take the mean of consecutive lots of three samples, there will be 1200 estimates of the mean wind speed, and the mean of those 1200 estimates will equal the mean of the entire 3600 sample for the whole hour. Large values of the three-second means are usually referred to as gusts, and the highest three-second mean

wind speed is referred to as the peak 3-second gust, in this case the maximum over the hour. The "gust factor" is then a theoretical conversion between an estimate of the mean wind speed, in this case for the hour, and the expected highest gust wind speed over the hour. The relevance of a gust factor is based on the implicit assumption that the flow is turbulent but the mean wind speed is steady or the wind field is stationary. In addition, the gust factor will be relevant only for a specific surface roughness, and also to vary with elevation, increasing towards the surface.

With this background we now proceed to describe the analysis methods.

3.1 Stationarity Test
We have tested the wind speed data for stationarity by applying the Run Test for various mean wind speeds over various durations. The Run Test involves a sequence of N observations of a random variable (mean wind speed estimates in this study), where each observation is classified into one of two mutually exclusive categories, identified by a plus (+) or minus (-), which may appear as follows

$$+ + - + + - + + + - + - - + - - + - - -$$
$$123456789101112$$

A run is defined as a sequence of identical observations that is followed and preceded by a different observation or no observation at all. In this example, there are $r = 12$ runs in a sequence of $N = 20$ observations. The number of runs that occur in a sequence of observations gives an indication as to whether or not results are independent random observations of the same random variable. Further, if the number of plus observations equals the number of minus observations, such as values above or below the median, then the sampling distribution of the number of runs in a sequence is a random variable, r, with a mean, μ_r, and variance, σ_r^2, as follows:

$$\mu_r = \frac{N}{2} + 1$$

$$\sigma_r^2 = \frac{N(N-2)}{4(N-1)}$$

The exact probability distribution can be derived from combinatorics (Brownlee, 1984), but it is cumbersome and in practice, a normal approximation is used for large values of N. Runs can be used to examine data for the existence of trends or in turn stationarity of samples. This can be performed by testing the hypothesis that there is no trend – i.e. that the sequence of N observations are independent, and therefore the number of plus observations equals the number of minus distributions and the number of runs in the sequence will have a known sampling distribution. The hypothesis can be tested at any desired level of significance, α, by comparing the observed runs to the interval between $r_{n;1-\alpha/2}$ and $r_{n;1-\alpha/2}$ where $a = N/2$. If the observed number of runs falls outside the interval, the hypothesis is rejected at the α level of significance; otherwise, it is accepted.

3.2 Analysis of Mean Wind Speeds
Mean wind speeds have been calculated from the scalar average over the interval of interest, except in the analysis of the Lutong tower profiles, where a 1-hour vector average was calculated, to be consistent with the vector average wind direction with which records were selected for analysis.

3.3 Spectral Estimation
We have followed the Welch (1967) method for estimating power spectra, in our case for sample records consisting of one hour of 1.0 Hz samples of wind speed. Records of one hour appear to be the duration most commonly considered for wave spectra (ISO, 2012, Forristall, 1988). Accordingly, we have segmenting the sample record into half-overlapped segments of 512 s, applied a Blackman-Harris 4-sample smoothing window (Harris, 1978), estimated the wind speed variance density spectrum for each segment using a FFT routine, and finally averaging the 13 separate variance density spectra.

Thus, our wind speed power spectra have a spectral resolution (and lowest frequency) of approximately 0.002 Hz, corresponding to a periodicity of around 8.5 minutes or 0.14 cycles/hour and a Nyquist frequency of 0.5 Hz, corresponding to a periodicity of 2 seconds or 0.00056 cycles/hour.

We compare non-dimensionalisations of these spectra against the forms proposed by Forristall (1988) for the so-called blunt spectrum and the ISO (2012) spectrum.

The blunt spectrum is defined by

$$\frac{fS(f,z)}{\sigma^2} = \frac{A\tilde{f}}{\left(1 + B\tilde{f}\right)^{5/3}} \tag{1}$$

where f is the frequency, S is the dimensional spectral density, σ^2 is the variance of the wind speed of the sample record, A and B are constants, which we set to the Forristall (2012) values of $A = 42$ and $B = 63$, and f is the non-dimensional frequency defined by

$$\tilde{f} = \frac{fz}{u} \tag{2}$$

where z is the elevation of the wind measurements and u is the 1-hour mean wind speed at elevation z.

The ISO (2012) spectrum, $S(f, z)$, is defined by

$$S(f, z) = \frac{320 \left(\frac{u_{10}}{10}\right)^2 \left(\frac{z}{10}\right)^{0.45}}{\left(1 + \tilde{f}_{\text{ISO}}^{0.468}\right)^{5/1.404}} \tag{3}$$

where u_{10} is the 1-hour mean wind speed in m/s at elevation 10 m, and $\tilde{f}_{\text{ISO}}$ is the non-dimensional frequency defined by

$$\tilde{f}_{\text{ISO}} = 172 \left(\frac{z}{10}\right)^{2/3} \left(\frac{u}{10}\right)^{-0.75} \tag{4}$$

4.0 Results
4.1 Stationarity
Our primary interest in wind stationarity is with the averaging intervals for mean wind speeds specified in design criteria and with the fundamental duration of one hour upon which the ISO scaling factors are based. Accordingly, we have tested for stationarity of 10-minute means, 1-minute means, and 3-second means over 1-hour durations. In addition, we have tested the 1 Hz data for stationarity over one hour, as this is the sample record duration that the wind speed power spectra are calculated.

The 1 Hz data for each location was divided into adjacent 1-hour sample records or segments of 3600 wind samples, making 744 such segments for each data set. Then for each of the 744 1-hour segments, the 3600 data were further divided into adjacent sub-segments of the given averaging interval – 10-minutes, 1-minute, and 3-seconds, and the data in each sub-segment were averaged. This resulted in 744 lots of 6, 60, 1200, and 3600 data to be tested for stationarity using the run test. Hourly segments that contained any invalid 1-second sample were ignored.

Table 1 presents the results, giving the percentage occurrence of stationary 1-hour segments, for wind speeds averaged over the subsegment durations of 1 s (not averaged), 3 s, 60 s, and 600 s. Thus, the number of subsegments in each 1-hour segment is 3600, 1200, 60, and 6 for respectively the 1 s, 3 s, 60 s, and 600 s mean wind speeds. The number of 1-hour segments in Table 1 corresponds to the number of 1-hour segments used in the analysis, that is those with 3600 good wind speed samples..

Surprisingly, the results show that there are no stationary 1-hour segments for the original 1 Hz data set and for the 3 s mean wind speeds, a relatively low percentage occurs for the 60 s means, and all the 600 s cases were deemed stationary with the runs test.

Location	Number of 1-hour segments	Sub-segment duration (s)			
		1	3	60	600
E11	695	0	0	3.4	100
F23	727	0	0	8.9	100
SF	702	0	0	15.4	100
Lutong 75 m	744	0	0	7.2	100
Lutong 57 m	744	0	0	9.9	100
Lutong 45 m	744	0	0	17.7	100
Lutong 33 m	744	0	0	20.8	100
Lutong 15 m	744	0	0	28.9	100

Table 1: Percentage occurrence of stationary 1-hour segments, for wind speeds averaged over sub-segment durations of 1-second (not averaged), 3 s, 60 s, and 600 s. The number of 1-hour segments corresponds to the number of 1-hour segments used in the analysis and are those with 3600 good wind speed samples.

Figure 1 gives examples of time series plots of the wind speed of two 1-hour sample records from the Lutong 75 m data set,

showing the 1 Hz samples (blue), 3-s means (green), 60-s means (red), 600-s means (black), and 1-hour mean (blue dashed). The 1-minute mean data are non-stationary in the upper plot but stationary in the lower plot. The 10-minute mean data are stationary in both examples, and the 1 Hz data and 3-second mean data are non-stationary in both.

The upper plot in Figure 1 is clearly non-stationary. Shortly after 1500 seconds, the wind speed increases and becomes more variable. This record is not expected to be stationary, not even for the 10-minute mean data, which show an increase from below the 1-hour mean to above it after the wind speed increases. Nevertheless, the run test determines that the 10-minute mean data in this record are stationary at the $\alpha = 0.05$ level of significance. This does not appear correct; a data set of six records and two runs might be expected to be stationary, and the fact that the run test does not indicate it to be so, demonstrates that there are too few data (6 in this case) to perform a sensible run test. In fact, a data set of 6 with two runs will always pass the test at the $\alpha = 0.05$ level.

The lower plot in Figure 1 appears more likely to be stationary. Nevertheless, the variability is apparently sufficient that neither the 1 Hz data nor the 3-second means are stationary. The fact that the 1 Hz samples and 3-second means are non-stationary in all cases is interesting and clearly casts doubt on the validity of stationarity implicitly assumed with the application of the gust factors and the calculation of power spectra. The 1-minute mean data in the lower plot are stationary according to the run test. Apparently, averaging over 1-minute removes the variability that caused the 1 Hz data and the 3-second data to fail the run test.
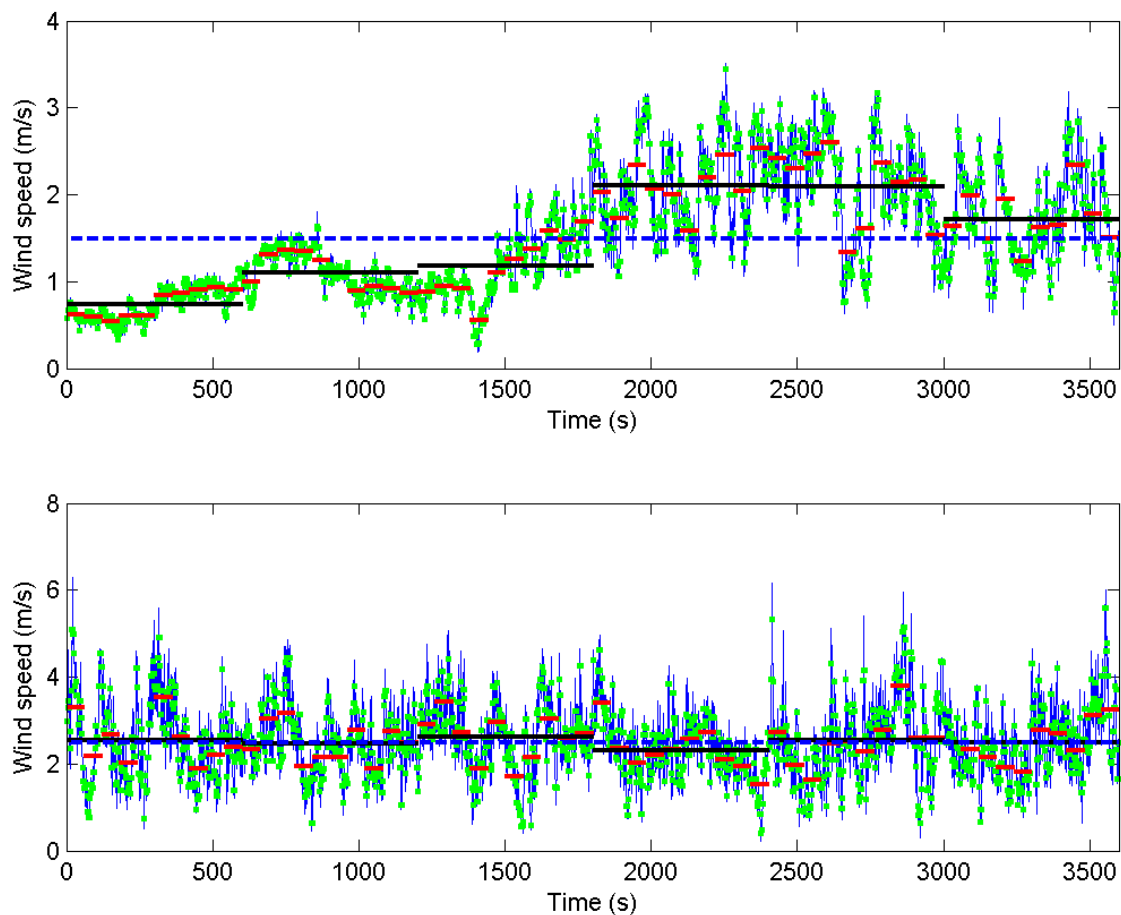

Figure 3: Time series plots of the wind speed of two 1-hour sample records from the Lutong 75 m data set, showing 1 Hz samples (blue), 3-s means (green), 60-s means (red), 600-s means (black), and 1-hour mean (blue dashed). The 1-minute mean data are non-stationary in the upper plot but stationary in the lower plot.

4.2 Mean Wind Speeds

Scatter plots of the ratio of the peak 3-second gust to the 60-minute mean wind speed against the 1-hour mean wind speed are given in Figure 4, for the eight data sets. The red dashed curves denote the range of the 95 percentiles. The continuous red curves are the 50 percentiles, and the black curve is the ISO gust ratios for the given elevation and 1-hour mean wind speeds. The percentiles are estimated only the range of 1-hour mean wind speed in which there is a large enough data to make a reliable estimate.

The data show a large range in the measured gust ratios. Both the ratio and the range of the ratio decreases with increasing 1-hour mean wind speed, consistent with the behaviour of the ISO gust ratio. However, apart from the trend, there is little agreement with the ISO gust factors. Although the ISO factors are generally within the 95 percentile range, the ISO factors over-estimate the measured gust factors at the higher elevations, and underestimate the measured gust factors at the lower elevations. Fortuitously, there is some agreement with the measured ratios for the Lutong measurements at 45m. It is also notable that the ISO gust ratios increase with elevation, an effect which is not observed in our data nor is it expected. In particular, the gust factors are expected to increase towards the surface; this effect is clear in the Lutong tower data, but a systematic increase in the gust factors with increasing elevation was measured in the data used to develop the ISO ralationships (Heggem, et al., 1991).

It should also be noted that there has been no pre-processing of our data, such as trend removal or selecting 1-hour segments that were less non-stationary, as would be possible from the run test results. By comparison, Heggem et al. (1991) selected only data with the 1-hour mean wind speed greater than 15 m/s and detrended their 1-hour records before analysis. There were no measurements with 1-hour mean wind speeds greater than 15 m/s in the data used in this study.
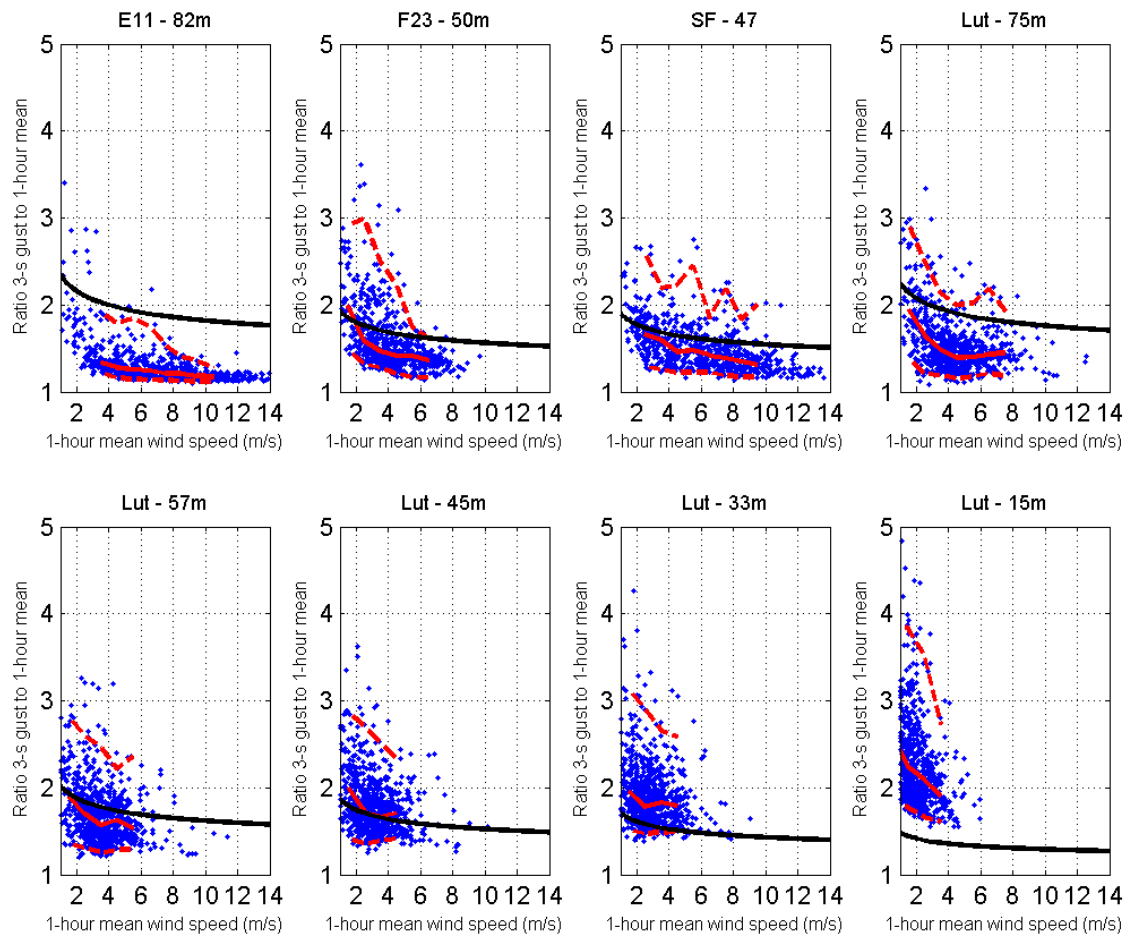

Figure 4. Scatter plots of the ratio of the peak 3-second gust to the 60-minute mean wind speed against the mean 1-hour wind

speed, for the eight data sets. The red dashed curves are denote the range of the 95 percentiles. The continuous red curves are the 50 percentiles, and the black curve is the ISO gust ratios for the given elevation and 1-hour mean wind speeds.

4.3 Wind Speed Profiles

Figure 5 shows 1-hour mean wind speed profiles measured at the Lutong tower (continuous curves) and the corresponding ISO profiles referenced at the 33 metre elevation. Profiles are given for the minimum wind speed, the 2.5, 50, and 97.5 percentiles, the maximum, and the mean of the wind speeds at all elevations. Records in which the 1-hour vector mean direction at all evelvations was within the sector [45,225] to reduce the effect of the wind effect of the nearby buildings. This resulted in 459 records or profiles for analysis.

With the exception of the very low wind speed cases (the minimum and 2.5 percentile cases) the measured profiles show a significantly larger shear than the corresponding ISO profiles. Even the mean profile, which is not an actual measured profile but gives information on the shape of the profiles in general, shows a much larger shear. Of course, the Lutong site is on land, albeit near the coast, with an expected increased surface roughness by comparison the measurements used to develop the ISO profiles, which were also made on land but near to the sea and at a site with a low surface roughness.
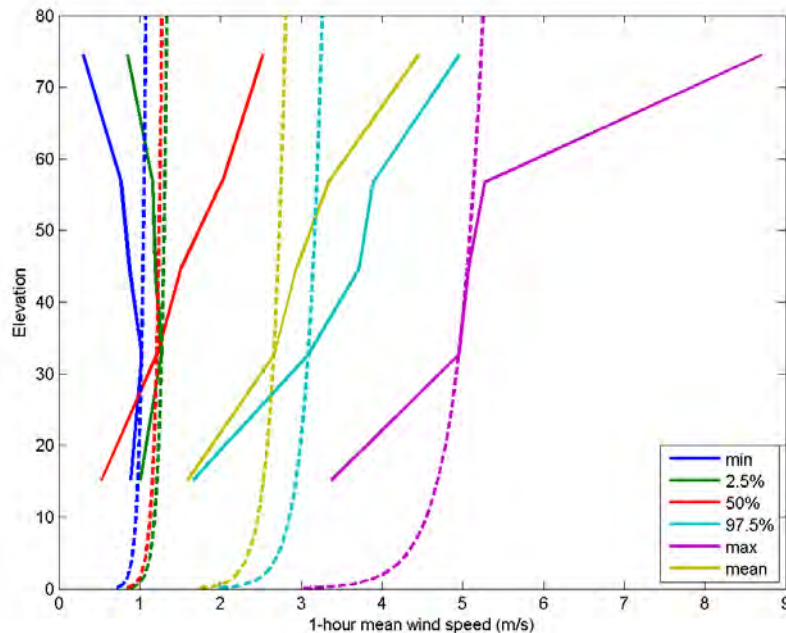

Figure 5: 1-hour mean wind speed profiles measured at the Lutong tower (continuous curves) and the corresponding ISO profiles referenced at the 33 metre elevation. Profiles are given for the minimum wind speed, the 2.5, 50, and 97.5 percentiles, the maximum, and the mean.

4.4 Wind Speed Spectra

The estimated non-dimensional spectra, fS/σ^2, with non-dimensional frequency defined by Equation (2), for each data set, are plotted in Figure 6. The red dashed curves denote the range of the 95 percentiles. The continuous red curves are the 50 percentiles, and the black curve is the Forristall blunt spectrum defined by Equation (1).

Just as we saw in the gust ratio data, the non-dimensional spectra show large variability. The spread in the spectra from the various sites is similar, but there are notable differences. A relatively large number of spectra for the F23, SF, and Lut − 75m data sets have peaks in the density at $\tilde{f} \sim 10$, while this is less obvious in the other data sets; spectra with low density at $\tilde{f} \sim 10$ are absent from the two offshore locations F23 and SF but present at the offshore location E11; and spectra with elevated densities at $\tilde{f} \sim 100$ exist at E11 in none of the other data sets.

For the most part, the Forristall blunt spectrum lies within the 95 percentiles of each data set, and with the exception of the F23 and SF data sets is similar to the 50 percentile curve in the data, while noting that the 50 percentile curve does not represent a specific spectrum.
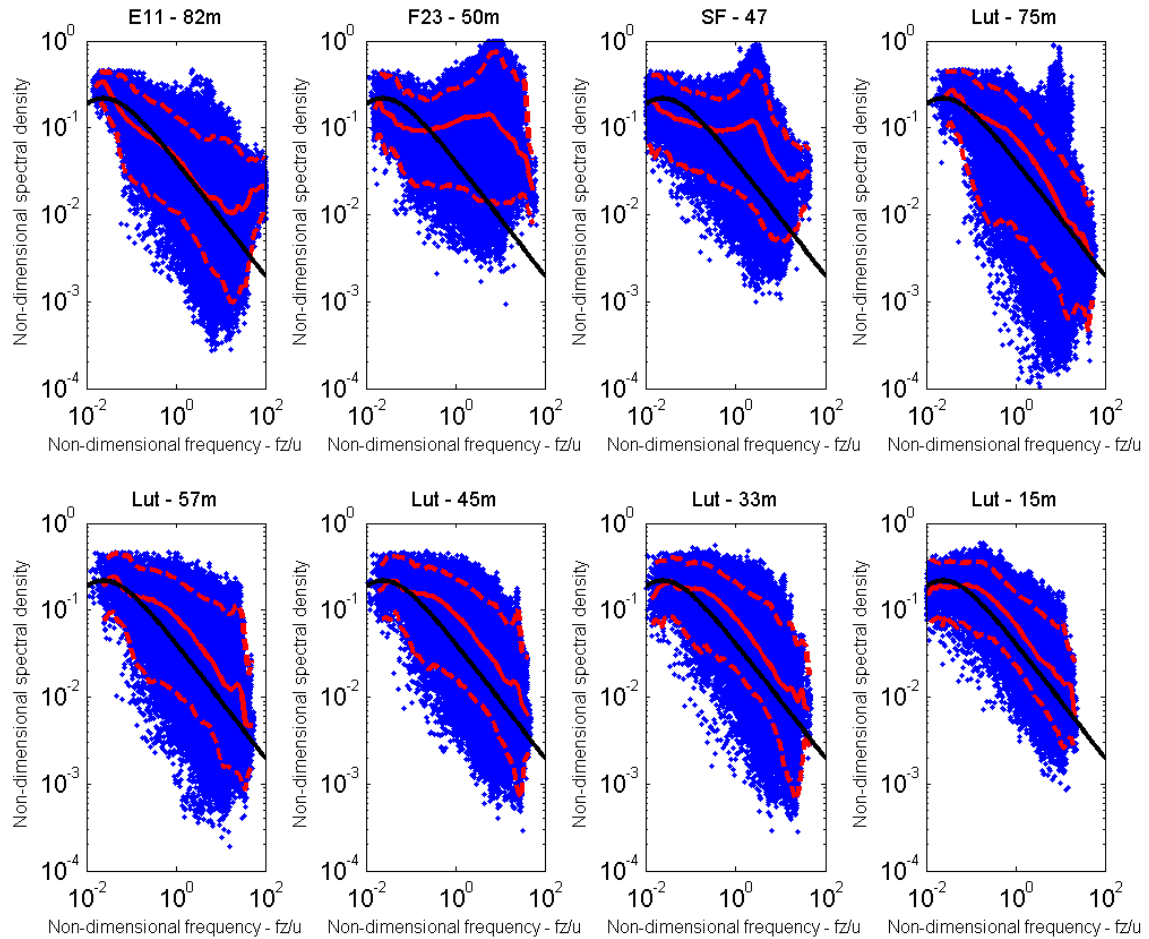
Figure 6: Non-dimensional spectra, fS/σ^2, with non-dimensional frequency defined by Equation (2), for each data set. The red dashed curves are denote the range of the 95 percentiles. The continuous red curves are the 50 percentiles, and the black curve is the Forristall blunt spectrum defined by Equation (1).

The estimated non-dimensional spectra, fS/σ^2, with non-dimensional frequency defined by Equation (4), for each data set, are plotted in Figure 7. The red dashed curves denote the range of the 95 percentiles. The continuous red curves are the 50 percentiles, and the black curve is the non-dimensional version of the ISO spectrum defined by Equation (3).

By comparison with the Forristall blunt spectrum, the non-dimensional ISO spectrum appear to agree better with the 50 percentile curve for the land-based Lut – 15m to Lut – 57m data sets; otherwise there is little to distinguish the relative agreement between the two spectral forms and the data.
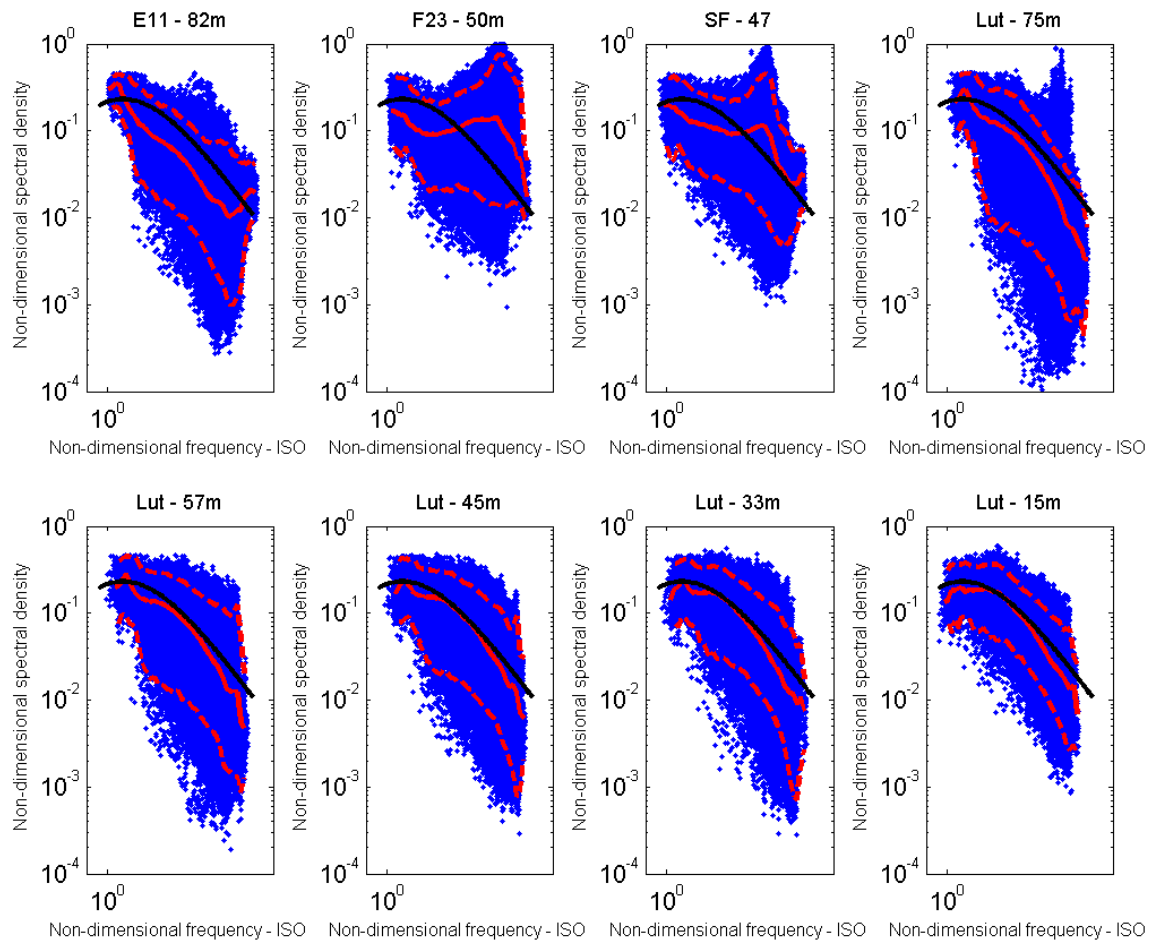
Figure 7: Non-dimensional spectra, fS/σ^2, with non-dimensional frequency defined by Equation (2), for each data set. The red dashed curves denote the range of the 95 percentiles. The continuous red curves are the 50 percentiles, and the black curve is the ISO spectrum defined by Equation (3) but non-dimensionalised.

Figure 8 present specific non-dimensional spectra for specific criteria for the Lut – 75m data set, to provide comparison against the two spectral forms. Spectra for the most non-stationary, the least non-stationary, the minimum 1-hour mean wind speed, and the maximum 1-hour mean wind speed are given the for the non-dimensional frequencies defined by Equation (2) (upper plots) and as defined by Equation (4) (lower plots).

The estimated spectra show broadly similar characteristics to the two spectral forms, but quite clearly, there is generally little agreement in the spectral levels. The spectral densities generally decrease with increasing frequency, and at high frequencies, all the spectra show a fairly constant roll-off with increasing frequency, similar to the two spectral forms. There is even a tendency for two of the examples – the least non-stationary and the maximum 1-hour mean wind speed to peak at low frequency as the two spectral forms do. It is also interesting to note that the best agreement between the estimated spectra and the functional forms is for the maximum 1-hour mean wind speed, suggesting a possible better match might be achieved for wind speeds approaching those for which the spectral forms were developed.
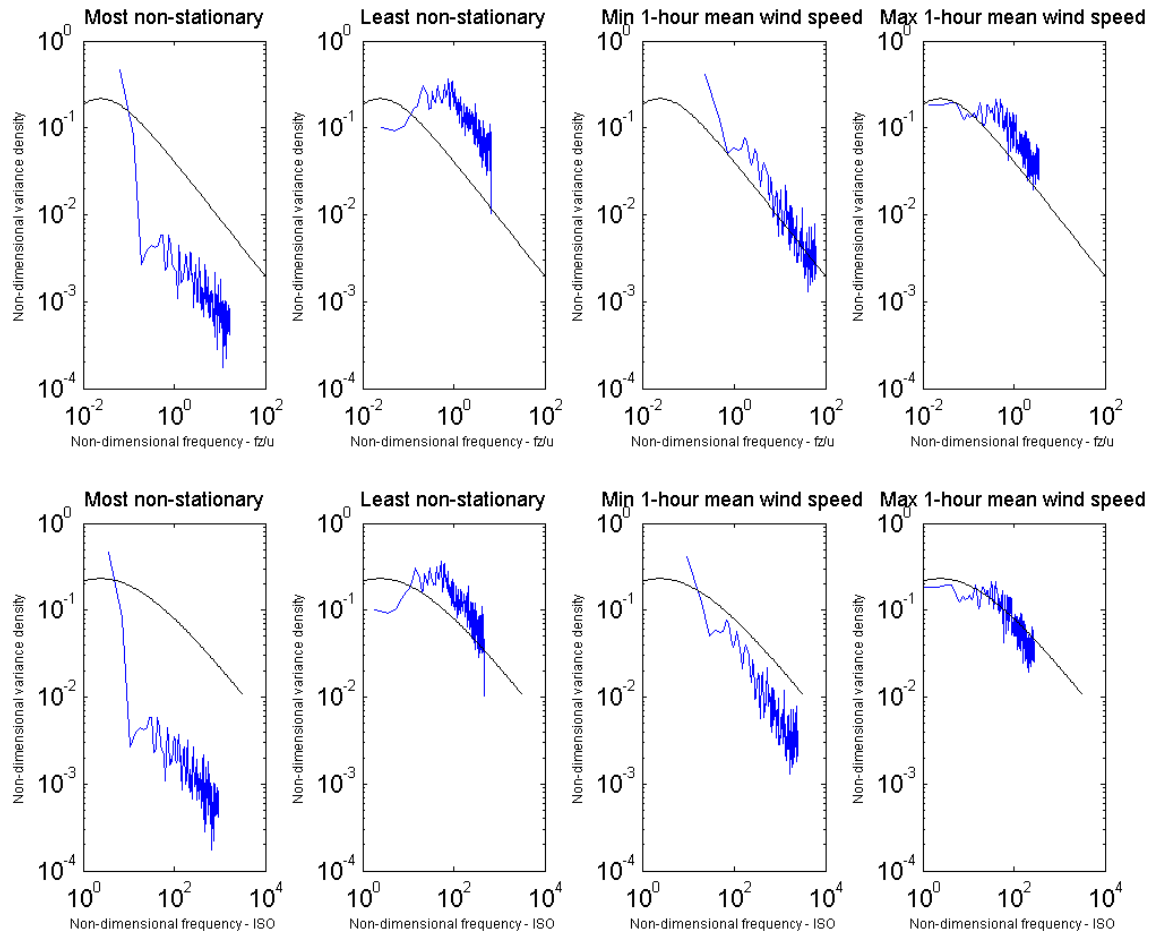
Figure 8: Examples of specific non-dimensional spectra for specific criteria for the Lut – 75m data set. Spectra for the most non-stationary, the least non-stationary, the minimum 1-hour mean wind speed, and the maximum 1-hour mean wind speed are given the for the non-dimensional frequencies defined by Equation (2) (upper plots) and as defined by Equation (4) (lower plots).

5.0 Conclusion

For the most part our wind data are not well described by the ISO relationships. Our 3-second gust to 1-hour mean speed factors are lower than the ISO values for our offshore locations. The ISO factors decrease with decreasing elevation, which is opposite to the trends in our data. The measured wind profiles show more shear than the ISO profiles. The ISO wind spectrum lies within the bulk of our data, but selected individual spectra show large departures; the comparisons against the Forristall blunt spectrum were similar.

It is acknowledged that the wind speeds in our data are much less than those that the ISO relationships were based on, but the differences between the tropical environment of our measurements and the mid-latitude climate that the ISO relationships are based on cannot be ignored. Our data were recorded when the northeast monsoon is active in the South China Sea. Thus, our data are representative of monsoonal conditions, and the largest wind speed events likely to be associated with squalls.

Our 1 Hz sample and 3-second average wind speeds are non-stationary over 1-hour periods, as are most (between 3.4% and 15.4%) of the 1-minute mean wind speeds. The number of stationary 1-minute mean wind speed records increases with decreasing elevation at the Lutong tower (7.2% at 75 m elevation to 28.9% at 15 m elevation).

The results are somewhat disconcerting. The degree to which the data are non-stationary and the general disagreement with the ISO relationships is surprising, and in particular puts into question the use of the ISO relationships for the region. Additional effort is needed to corroborate these findings, and if necessary provide more appropriate wind relationships for design in the region. Our measured wind data is substantial and can be used as a basis for a more comprehensive study than has been possible for this paper.

References

API 2007: Recommended practice for planning, designing and constructing fixed offshore platforms—working stress design (RP 2A-WSD). American Petroleum Institute.

Brownlee, K.A., 1984: Statistical Theory and Methodology In Science and Engineering. 2nd Ed., Robert E. Krieger Publishing Company, Inc. Malabar, Florida.

Forristall, G. Z., 1988: Wind spectra and gust factors over water. *Proceedings of the 20th Annual Offshore Technology Conference*, Houston, OTC 5735.

Harper, B. A., Kepert, J. D., and J. D. Ginger 2009: Guidelines for converting between various wind averaging periods in tropical cyclone conditions, World Meteorological Organisation, Sixth Tropical Cyclone RSMCs/TCWCs Technical Coordination Meeting, Brisbane Australia, 2-5 November.

Harris, F. J., 1978: On the use of windows for harmonic analysis with the discrete Fourier transform. *Proc. IEEE*, **60**, No. 1, 51-83.

Heggem, T., Lovseth, J., Mollestad, K., Aasen, S., and O. Anderson, 1991: The maritime turbulent wind field measurements and models. Final report for the Statoil Joint Industry Project. Allforsk AVH, Department of Physics, Dragvoll, Norway.

ISO, 2012: Petroleum and natural gas industries — specific requirements for offshore structures — part 1: metocean design and operating conditions. International Organization for Standardization, ISO TC 67/SC 7, Date: 2012-02-10, ISO/DIS 19901-1, ISO TC 67/SC 7/WG 3.

Van der Hoven I., 1957: Power spectrum of horizontal wind speed in the frequency range from 0.0007 to 900 cycles per hour. *J. Meteorology*, **14**, 160-164.

Welch, P. D., 1967: The use of fast Fourier transform for the estimation of power spectra: A method based on time averaging over short modified periodograms. *IEEE Trans. Audio Electroacoust.*, **AU-15**, 70-73.